Blazar Polarimetry with the ROVOR Telescope

Parkes Whipple

A capstone report submitted to the faculty of
Brigham Young University
in partial fulfillment of the requirements for the degree of

Bachelor of Science

J. Ward Moody, Advisor

Department of Physics and Astronomy

Brigham Young University

July 2017

ABSTRACT

Blazar Polarimetry with the ROVOR Telescope

Parkes Whipple
Department of Physics and Astronomy, BYU
Bachelor of Science

Four linearly polarized filters, at 0°, 45°, 90° and 135° with respect to north, are calibrated for the ROVOR telescope in Delta, UT. Standard non-polarized stars are used to determine the differences in throughput between the four filters. The throughput is found to be equal to within 1%. Standard polarized stars are used to determine the accuracy of the degree of polarization and the offset between the true position angle and our measured position angle. The amplitude, or degree, of polarization is accurate to within 0.5 percentage points. The offset between our *instrumental* position angle and the *true* value is found and is given by $true = 0.4499(instr) + 47.322$ with an R^2 value of 0.9997. We are confident of the position angle to within 3°. ROVOR is now calibrated and ready to continue polarimetric observations.

Keywords: [Polarimetry, Calibration, Blazar, Quasar, ROVOR]

Contents

Chapter 1

Introduction

1.1 Background

The blazar community is interested in the polarization of astrophysical jets, especially as it compares to blazar flaring. The Air Force is also interested in polarization for research on geosynchronous satellites. For both needs, it is to our advantage to develop a method for measuring polarization if we want to be a participant in this type of research. This research is still in the proof-of-concept phase but is generating some interest.

The 0.4m ROVOR telescope in Delta, Utah is a BYU-owned observatory. The acronym stands for Remote Observatory for Variable Object Research. It has been in operation for eight years and has been a research tool leading to seven publications from BYU students under Dr. Moody's supervision. It has been an especially great tool for photometry of blazars, which are quasars with a jet aimed at Earth. A large survey project is underway on photometric observations for 180 blazar galaxies to determine how often they flare in brightness.

Polarimetric calibration is the next step for ROVOR to contribute to the astronomical community and especially the study of blazar galaxies. One source of blazar radiation is synchrotron radiation

from the accreting matter around the black hole and the related magnetic field. It has been proven that synchrotron radiation is polarized (Westfold 1959). More recent research has shown the importance of how polarization relates to radiation intensity and how it informs our models of active galaxies (e.g. Angelakis et al. (2016); Blinov et al. (2015); Joshi, Marscher, & Böttcher (2016); Larionov et al. (2016)).

1.2 Motivation

There is recent evidence that optical flaring of blazars coincides with changes in polarization. Sorcia et al. (2014) reports a large rotation in polarization angle after a flaring period. A 90° rotation is reported by Myserlis et al. (2016) right before a flaring period begins. The research is on-going and not yet definitive as to the relation between polarization and blazar flaring. These studies seek to validate or debunk magnetohydrodynamic models for blazar and quasar interiors. The unified model of quasars is being refined by polarimetric measurements. The ROVOR team, and the BYU astronomy program generally, seek to be at the forefront of the field. We believe this is the best step to appeal to global partners and finance future projects.

1.3 Context

In 2016, four linearly polarized filters from Edmund Scientific were installed in ROVOR by Dr. Moody. Following the standard of the field, they were oriented with respect to north (Fossati et al. 2007). Despite great care, the precision of the alignment was unknown. The ROVOR team was successful in demonstrating the potential of this system when the Air Force asked for a system to find the geometry of a man-made satellite by mapping the polarization against the satellite's angle with the sun (See Figure 1.1). The sun's reflection off the satellite panels polarizes the incident ray. The amount of polarized light indicates the size of the satellite panel. This proof of concept

was differential in nature, comparing the intensity between different filters so it did not require a calibrated system to determine the actual maximum angle of polarization, also called position angle. It was a hopeful moment to see the usefulness of having a polarimeter.

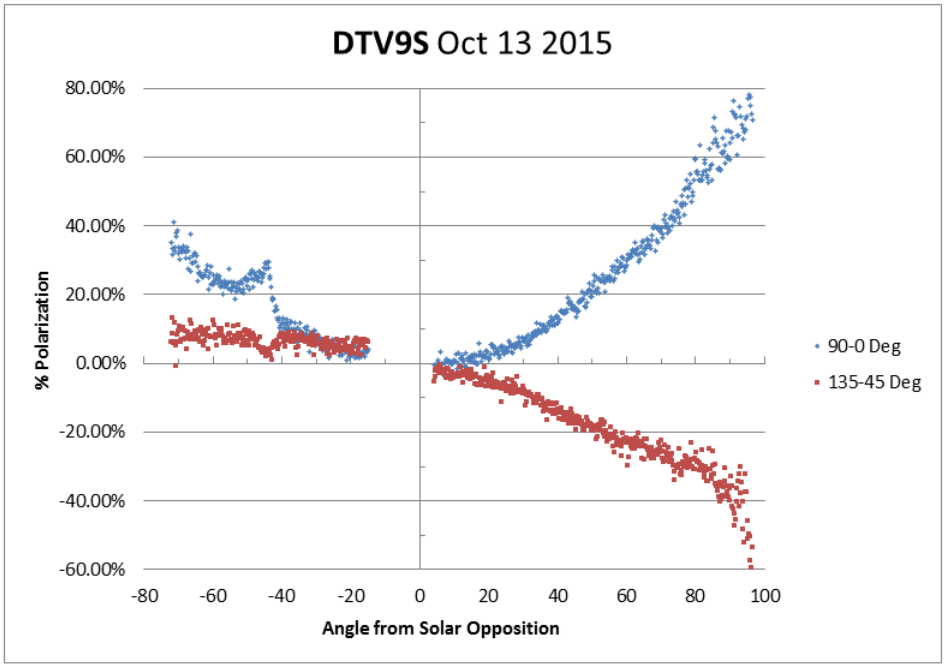

Figure 1.1 The polarization of satellite DTV9S on October 13, 2015. The x-axis corresponds to time of night with evening on the left and morning on the right. The gap in data is when the satellite was eclipsed by Earth's shadow. The plot presents the percentage difference between the two filters of each orthogonal pair: 90° & 0° and 135° & 45°. The plot shows that the polarization magnitude and plane changes dramatically through the night. It should be possible to develop a unique signature for each satellite type that can be used to identify satellites and monitor their aging.

The ROVOR team has also been involved in the Whole Earth Blazar Telescope (WEBT), which is a conglomerate of blazar astronomers that operate global campaigns to observe flaring periods

of active galaxies. This cooperation allows for more complete light curves since the object can be observed continuously as night time passes around the globe. BYU students and faculty have contributed to that data collection and are found as authors on the resulting papers. Increasingly common have been requests for polarimetric data in conjunction with the photometric data. To contribute to more papers and greater understanding of these active galactic nuclei, it became necessary to calibrate the polarized filters and offer a true position angle for the polarized light.

Chapter 2

Observations

Observations for this project were taken between 10 April and 3 June 2017. The exceptional weather requirements for polarimetry, discussed in the next chapter, spread out the observing timeline. Because ROVOR is a remote observing site, the following sections explain how the observations are set up and executed through software on a remotely operated computer at the telescope site.

2.1 Preparing to Observe

Polarimetric standards have been calibrated for general use by the Subaru FOCAS team. We used four polarized standards from a popular list used by the Subaru telescope; they are also known as Serkowski standards (Gehrels 1974; Serkowski et al. 1975). Their published standards include the object identifier and stellar coordinates, Right Ascension (RA) and Declination (δ), as well as the percentage of polarization and polarization angle. It is possible to obtain the altitude of a star using spherical trigonometric equations and the definition of RA.

Observing with ROVOR requires knowing when each star is visible in the desired ± 3 hour

hour-angle window. I found hour angle in the following manner. To solve for the altitude (a) we used the well-written notes of Dr. Eric Hintz at BYU. The zenith angle (z) is the compliment of the alititude: $a = 90^\circ - z$.

The zenith angle, z, can be defined by the following: $cos(z) = sin(\delta)sin(\phi) + cos(\delta)cos(\phi)cos(HA)$ where ϕ is the local latitude and HA is the hour angle. The hour angle is defined in terms of the RA and the Local Sidereal Time (LST): $HA = LST - RA$. The local time can easily be converted to LST through online tables or programs. To find the altitude of a particular star at a particular time, the equation can be written as: $a = 90^\circ - arccos[sin(\delta)sin(\phi) + cos(\delta)cos(\phi)cos(LST - RA)]$.

This is the more rigorous and involved method. An alternative method was used more often for this project. Using the online Neave Planetarium, the altitude of a nearby star was found and used to find the approximate altitude of the target object. With this, we can know what time to observe the target object. We observed no earlier than astronomical twilight, which can be found in tables online.

The telescope is housed in a small structure with a removable roof. This setup avoids the complications of creating a dome that can track with the sky, but leaves the telescope more susceptible to the elements when open. We use an outdoor camera to verify the weather before opening the roof and never observe if winds are above 20mph. The motor that opens and closes the roof is connected to a LabVIEW program, so it can be controlled remotely.

2.2 Using TheSkyX

TheSkyX is an astronomy program that communicates with the telescope equipment directly. A companion program called Orchestrate allows the user to enter a series of commands to run in sequence through the night. Once the observing hours are figured out for each target, we create the Orchestrate script to observe at the correct times with the correct filter. We take twilight flat fields, darks and biases as part of the series each night. Orchestrate has not been updated along with TheSkyX, so there are some lapses in capability. The Bias frame mode and the Flat frame mode must be changed manually in TheSkyX, while the Light and Dark frame modes can be scripted through Orchestrate.

The coordination between equipment and software make observing very easy through this remote setup. We connected to the computer on-siite through the RealVNC or TightVNC programs. Once the script was written and the programs activated, the observing began with a single click. It is most practical to create the script on a large screen, but it was often more convenient to begin the script through a VNC cell-phone app.

Chapter 3

Methods

Polarimetry requires ideal sky conditions. Unlike with photometry, there is no differential method because clouds change the polarization rather than simply reduce the intensity. Moonless nights are not necessarily required because moonlight has less of an impact on polarization.

Each frame was reduced using standard procedures and the CCD counts were obtained in the Mirametrics software. The photometry in Mira requires only one aperture on the target, making it less tedious than differential photometry. The values were copied into Excel for analysis. The following two steps use Mira and Excel.

3.1 Filter Throughput

The four filters were purchased from Edmund Optics. We had no reason to initially suspect they would transmit differently, since they were cut from the same sheet of polymer. But to be certain, we observed five non-polarized standard stars to compare the intensity through each filter. The standards were obtained from the Subaru FOCAS list which they use for calibration. These are plotted in Figure 3.1. The plot of filter intensities showed no consistent trend across filter which indicates that there was no significant transmission difference between the four polarizers. If a

particular filter were found to be consistently higher or lower than the rest, it would need to be manually equalized to the others before the next step of analysis. Since this was not the case, no correction was necessary.

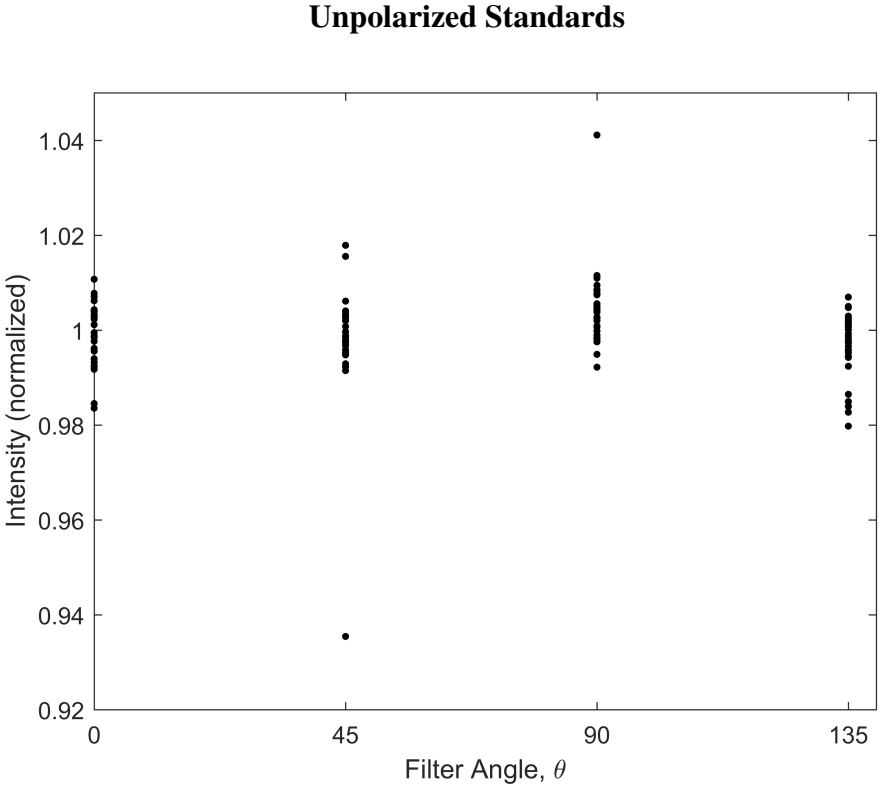

Figure 3.1 These five stars have no polarization. The intensities are normalized and no filter is biased up or down, so there is no need to account for differences in transmission. They are equal to within the precision we need.

3.2 Calibration Offset

The primary goal of this exercise is to find the relationship between our measured value of polarization angle and the true value. The amount and angle of polarization is found through the following method.

The angle of polarization, or position angle, will be the focus. In Excel, they are plotted with the following sine fit: $f(\theta) = A \cdot sin(2\theta + \phi) + 1$. The amount of polarization is given by the value A. The instrumental angle of polarization is given by the phase of the sine fit, ϕ. It is shifted up by 1 to match the normalization. The four points on the left half of each plot come from the filter's average value, given by Mira. The right half of the plot is copied from left.

We used a basic least-squares fit method to optimize the sine fit. We took the difference between the filter intensity and the fit at that point, then summed the differences and squared them.To match the R^2 value from Excel, we also took the square root and subtracted it from 1. Our R^2 function in Excel looked like this: $1 - \sqrt{(I_0 - f(0))^2 + (I_{45} - f(45))^2 + (I_{90} - f(90))^2 + (I_{135} - f(135))^2}$. The values of ϕ and A were adjusted manually until the R^2 value was minimized.

The accuracy of the fit suggests the filters are oriented correctly (45° from each other). We would expect one value to be consistently outside the fit if the filters were not oriented correctly. The error for each parameter based on the fit is about 0.2 percentage points for amplitude and less than 1° for the phase. Despite the close fit on each plot, the ϕ and A values differ between plots for the same object. The standard deviations for ϕ vary between 2.5° and 4.5°. We would not expect precision better than 5° based on that error. The fits for each standard are shown below.

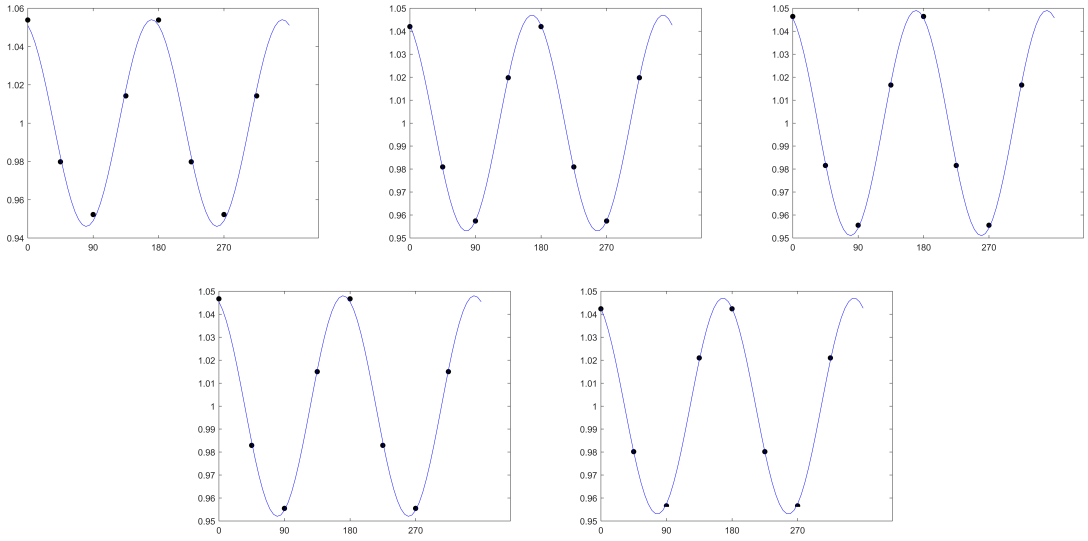

Figure 3.2 BD+64 106: $\bar{\phi} = 112°$, $\bar{A} = 4.9\%$, $\bar{R}^2 = 0.99746$

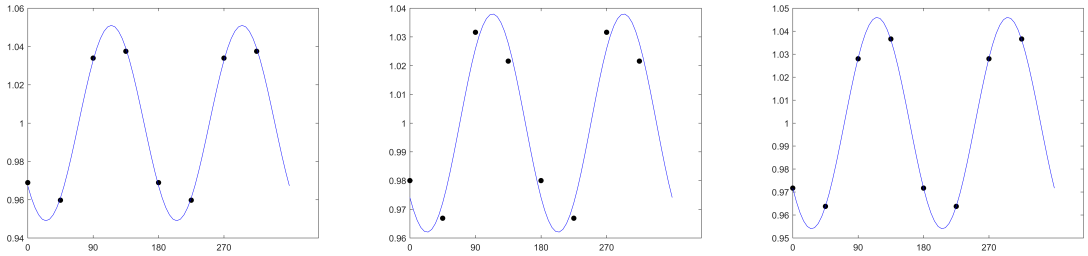

Figure 3.3 HD 251204: $\bar{\phi} = 220°$, $\bar{A} = 4.5\%$, $\bar{R}^2 = 0.99503$

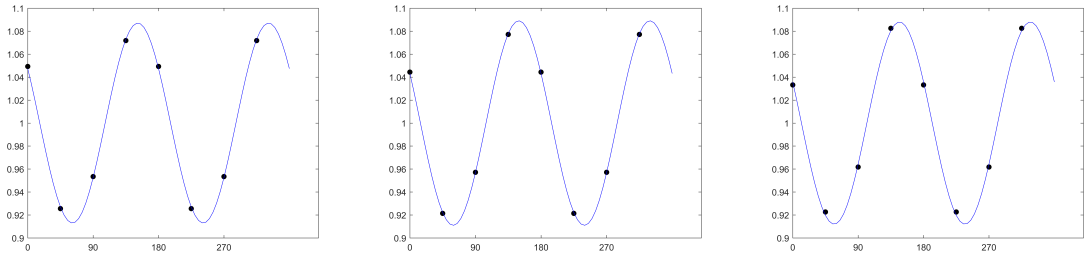

Figure 3.4 VI Cyg #12: $\bar{\phi} = 115°$, $\bar{A} = 8.8\%$, $\bar{R}^2 = 0.99683$

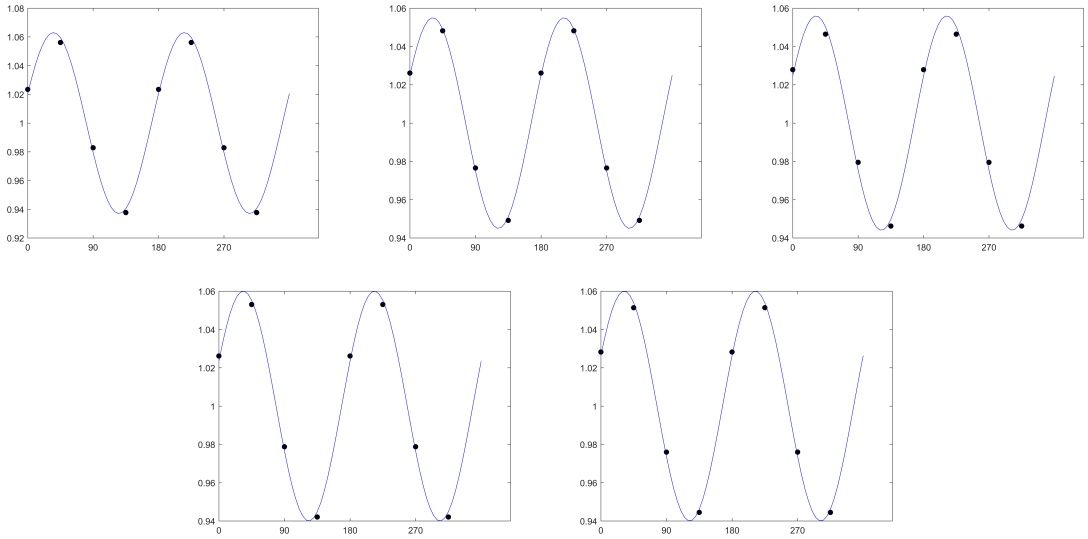

Figure 3.5 HD 204827: $\bar{\phi} = 24°$, $\bar{A} = 5.9\%$, $\bar{R}^2 = 0.99488$

Chapter 4

Results & Discussion

With 3-5 nights of data for each polarized standard, we found the average angle of polarization for each object. The accuracy of the sine fit inspires confidence in the data and we are pleased with the relative accuracy of the amplitude measurement. Our observed amplitudes are within 1 percentage point of the standards. The standard practice for polarimetry is to orient the first linear polarizer with respect to north. It is common to have an offset from the standard zero point because of filter alignment. Our expectation was to find a single offset value for (*standard-observed*). Instead, a plot of the instrumental value vs the standard value shows a linear relationship: $standard = 0.4499(observed) + 47.322$. Figure 4.1 shows the linear fit through the four points. The linear fit is extremely accurate. The R^2 value given by Excel is 0.9997.

Our method of using four filters spanning 180° has proven to be successful for finding the angle of linear polarization. The slope of our fit being very close to $1/2$ has revealed a conventional mismatch. While it is mathematically significant to consider a full 360° space, it is physically insignificant to consider more than 180°. For EM waves, a 45° oscillation is synonymous with an oscillation at 225°. Because of this physical situation, it is convention for polarization standards to never exceed 180°. When four linear polarizers are used, it is usually at intervals of 22.5° spanning 90°. Our setup covers 360° of phase space while the standard arrangement only covers 180° of

phase space. As shown, our arrangement is valid and will provide reliable results. The slope of 0.4499 (close to 0.5) in our fit is indicative of the conventional differences between the physics and a mathematical approach.

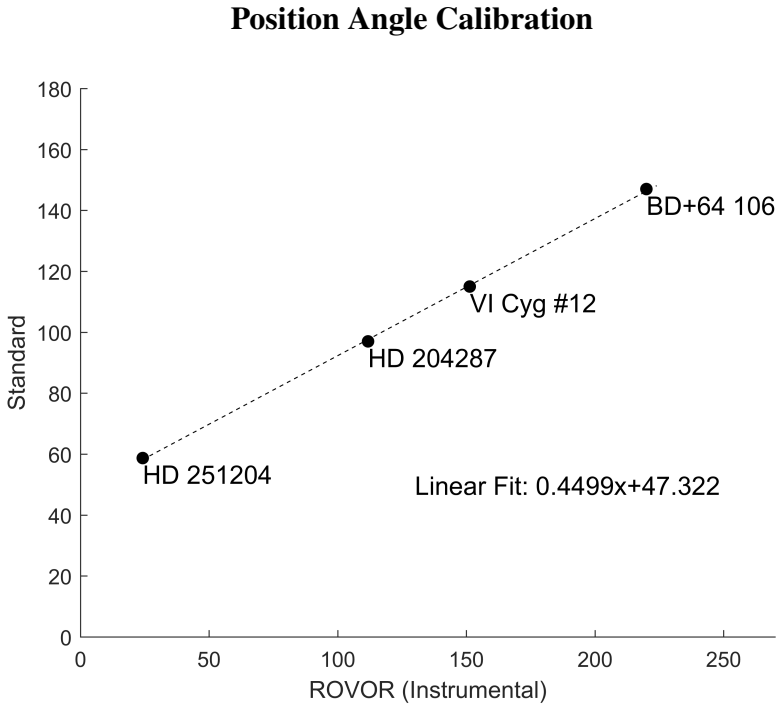

Figure 4.1 The instrumental position angle is plotted against the standard position angle for four stars. The relationship is almost perfectly linear.

Chapter 5

Acknowledgements

We acknowledge the Brigham Young University Department of Physics and Astronomy. We also acknowledge Dr. Sadun for helping ROVOR join a global community. We also wish to thank Neave Interactive Ltd. and their virtual planetarium for helping with the timing of observations.

Appendix A

Subaru FOCAS Polarization Standards

Polarized Standards

Star	RA(J2000)	δ(J2000)	Mag.	Sp Class	Amount of Pol (%)	Pol Angle (°)	Ref.
BD+64d106	00 57 36.7	+64 51 27	10.3	B1V	5.69+-0.04	96.6+-0.2	Sch92
HD 7927	01 20 04.9	+58 13 54	5	F0Ia	3.32+-0.04	92.1+-0.2	Wol96
BD+59d389	02 02 42.1	+60 15 27	9.1	F0Ib	6.70+-0.2	98.1+-0.1	Sch92
HD 19820	03 14 05.4	+59 33 48	7.1	O9IV	4.82+-0.03	115.4+-0.3	Wol96
HD 25443	04 06 08.1	+62 06 07	6.8	B0III	5.15+-0.03	135.1+-0.2	Wol96
HD 251204	06 05 05.7	+23 23 39	10.3	B0IV	4.04+-0.07	147	Tur90
HD 43384	06 16 58.7	+23 44 27	6.3	B3Ib	2.94+-0.04	169.8+-0.7	Hsu82
HD 154445	17 05 32.2	-00 53 32	5.6	B1V	3.67+-0.05	88.6+-0.7	Wol96
HD 155197	17 10 15.6	-04 50 03	9.2	A0	4.38+-0.03	103.2	Tur90
HD 161056	17 43 47.0	-07 04 46	6.3	B1.5V	4.00+-0.01	66.3+-0.3	Wol96
Hiltner 960	20 23 28.4	+39 20 56	10.6	B0V	5.66+-0.02	54.8+-0.1	Sch92
VI Cyg #12	20 32 40.9	+41 14 26	11.5	B5Ia	8.95+-0.09	115.0+-0.3	Sch92
HD 204827	21 28 57.7	+58 44 24	7.9	B0V	5.34+-0.02	58.7+-0.4	Wol96

Unpolarized Standards

Star	RA(J2000)	δ(J2000)	Mag.	Sp Class	Amount of Pol (%)	Pol Angle (°)	Ref.
Beta Cas	00 09 10.7	+59 08 59	2.3	F2III	0.04+-0.02	72.5	Sch92
HD 12021	01 57 56.1	-02 05 58	8.9	B7	0.08+-0.02	160.1	Sch92
HD 14069	02 16 45,2	+07 41 11	9	A0	0.02+-0.02	156.6	Sch92
HD 21447	03 30 00.2	+55 27 07	5.1	A1IV	0.05+-0.02	171.5	Sch92
G191B2B	05 05 30.6	+52 49 54	11.8	DA1	0.06+-0.04	147.7	Sch92
HD 94851	10 56 44.2	-20 39 52	9.2	B9	0.06+-0.02(B)	—	Tur90
GD 319	12 50 04.5	+55 06 03	12.3	DA	0.09+-0.09	140.2	Sch90
Gamma Boo	14 32 04.7	+38 18 30	3	A7III	0.07+-0.02	21.3	Sch92
HD 154892	17 07 41.4	+15 12 38	8	F8V	0.05+-0.03(B)	—	Tur90
BD+32d3739	20 12 02.1	+32 47 44	9.3	A6V	0.03+-0.02	35.8	Sch92
BD+28D4211	21 51 11.1	+28 51 52	10.5	oP	0.05+-0.03	54.2	sCH92
HD 212311	22 21 58.6	+56 31 53	8.1	A0V	0.03+-0.02	51	Sch92
Zeta Peg	22 41 27.7	+10 49 53	3.4	B8III	0.05+-0.02	40	Sch92

Bibliography

Angelakis, E., et al. 2016, MNRAS, 463, 3365

Blinov, D., et al. 2015, MNRAS, 453, 1669

Fossati, L., et al. 2007, PASP, 364

Gehrels, T., ed. 1974, Planets, Stars and Nebulae studied with photopolarimetry (Tucson, AZ: University of Arizona Press), 170

Joshi, M., Marscher, A., & Böttcher, M. 2016, Galaxies, 4(4), 45

Larionov, V., et al. 2016, Galaxies, 4(4), 43

Myserlis, I., et al. 2016, Galaxies, 4, 58

Serkowski, K., et al. 1975, ApJ, 196, 261

Sorcia, M., et al. 2014, ApJ, 794, 54

Westfold, K. 1959, ApJ, 130, 241